HYPERFINE STRUCTURE MEASUREMENT OF SODIUM A TOMIC-BEAM ORTHOGONALLY WITH DYE LASER R6G

Mohammed T. Hussein, *Zaidun A. Hafidh

Department of Physics, College of science, University of Baghdad. Baghdad- Iraq.
*Department of Laser and Optoelectronics Engineering, College of Engineering, University of A l Nahrain. Baghdad- Iraq.

Abstract

Sodium atomic beam of limited broadening, of angular divergence of 5.15^o was generated to investigate the hyperfine structure of sodium D_2 line. R6G dye laser was orthogonally interact with Na-atomic beam and recording of fluorescence signal (λ=5896Å) showed a hyperfine structure of Na-D_2 line of 1.03 GHz.

قياس التركيب الطيفي الدقيق لحزمة الصوديوم الذرية المتعامدة مع ليزر الصبغة نوع الرودمين R6G

محمد تقي حسين، *زيدون أحمد حافظ

قسم الفيزياء، كلية العلوم، جامعة بغداد. العراق-بغداد.

*قسم هندسة الليزر والالكترونيات البصرية، كلية الهندسة، جامعة النهرين، العراق-بغداد.

الخلاصة

تم توليد حزمة ذرية ضيقة (محدودة الاتساع) لبخار الصوديوم حيث كانت زاوية الانفراجية للحزمة بحدود (5.15) درجة، وذلك لقياس التركيب الشديد الدقة لمستويات الطاقة للصوديوم في خطي D_2. حيث تم استخدام ليزر الصبغة R6G للتداخل عمودياً مع حزمة الصوديوم حيث تم تسجيل خط طيف الفلورة للصوديوم عند (λ=5896Å). ويوضح التركيب الدقيق لخطي الصوديوم بعرض 1.03 كيكاهرتز.

Introduction

Atomic and molecular beams have been studied since their ties for the generation of limited divergence atomic or molecular beam for gases or vapour [1, 4].

The literature mostly includes the generation of an atomic beam from an oven by effusion from a slit to a less pressure boundary. The slit has to be of the order of the mean free path of the heated element as obtained from the P-T curve in the case of evaporation from solids or liquids. The beam is then generated according to Figure 1.

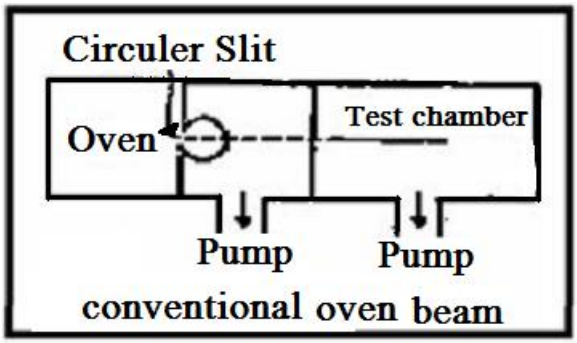

Figure 1: Shape of beam effusive

Where the divergence takes a cosine distribution. The beam is collimated by further insertion of slits which would also limits the net flux of

the beam. The maximum beam flux from effusive sources, reaches the order of 10^{10}part/sec steradian which makes it a source of limited yield [4].

The unresisted need to generate sources of high flux, minimum divergence and high speed throughputs has been attempted to comply with the above requirements. Nozzles have intense yield that vary between 10^{14}-10^{16} part/sec steradian and with limited divergence of the atomic or molecular beam. The velocity distribution of the beam reduces with super atomic or molecular beam from gases, but the literature has a little information about the generation of supersonic beam by evaporating metals [5].

This article presents the endeavour to design a nozzle for the generation of supersonic atomic beam obtained with sodium metal.

Theory and Design

The basic concept of fluid dynamic [1] and aerodynamics theory as explained by T.V on Karman 1954, contains the mean features for the explanation and formulation of fluid flow and nozzle design.

The main requirements for the fulfillment of supersonic flow are as follows [3, 4]:

1. Frictionless flow

The surface smoothness for the nozzle and temperature distribution where the skin friction of viscosity of the fluid and the rate of which the velocity increases above the surface.

2. Steady flow

No surface protrusions (sharp ends) that might cause disturbances which results in a shock wave formation [5].

3. Continuum flow

To obtain a continuous stream of atoms or molecules through the nozzle, the throat diameter of the nozzle should be much larger than the mean free path of the particles (λ_{mfp}).

$$\phi >> \lambda_{mfp}$$

$$\lambda_{mfp} = \frac{1}{\sqrt{2n\pi\sigma^2}} \quad \text{.....(1)}$$

where

ϕ = nozzle throat diameter

n = density of particles

σ = molecular collision diameter=3.72×10^{-8} cm for sodium at room temperature [4].

4. Adiabatic flow

Conditions are near to ideal case where no friction nor heat or gain into the system [5].

The equations of isentropic flow states.

γ= 1.4 diatomic molecules

γ = 1.667 monoatomic molecules

$$T/T_o = (P/P_o)^{\frac{\gamma-1}{\gamma}} \quad \text{.....(2)}$$

$$n/n_o = (P/P_o)^{\frac{1}{\gamma}} \quad \text{.....(3)}$$

$$\upsilon = \frac{1}{\left(1+\frac{\gamma-1}{2}M^2\right)^{1/2}}(\gamma T_o R)^{1/2} \quad \text{.....(4)}$$

$$A_e/A_o = \frac{1}{M}\left[\left(\frac{2}{\gamma+1}(1+\frac{\gamma-1}{2}M^2\right)\right]^{\frac{\gamma+1}{2(\gamma-1)}} \quad \text{..(5)}$$

J=nυ. Area of skimmer. Solid part/sec.

Where:

γ=ratio of specific heat

P=pressure outside nozzle

P_o=pressure inside nozzle container

T=temperature outside (downstream)

T_o=temperature inside nozzle container

n=density downstream

n_o=density inside nozzle container

M=mach no. :A_e=area of exit

A_o=throat area of nozzle

$$R = \frac{8.314 x 10^7}{\text{molecular weight}} \quad \text{erg/degree}$$

The main feature of the nozzle design is to start with the following [3, 5]

1. Desides the mass flow through the throat of the nozzle according to the pumps available that can handle this throughput.
   Gas density, velocity, a throat = mass flow = constant.
2. Desides a certain mach and work out of the ratio P/P_o, A/A_o and T/T_o.
   The final shape of the nozzle is obtained by trial and error due to other unknown parameters, like friction between vapour and surface of the nozzle. The final throat temperature should be higher than vaopur temperature to avoid condensation or shock wave formation.
3. The divergence angle of the nozzle (exit) has to satisfy two main requirements.
   a. Controlled slow expansion of the beam at the exit to avoid sudden expansion or shock wave formation [6].
   b. Jet boundary has to fulfill parallel flow (minimum divergence) where the pressure of the beam has to be equal to the pressure in the rest of the chamber.

$P_{jet}=P_{chamber}$ If otherwise

$P_j>P_C$ beam is over-expanded

$P_j<P_C$ beam is under-expanded, and in both cases the beam does not take parallel flow as shown in (Figure 2).

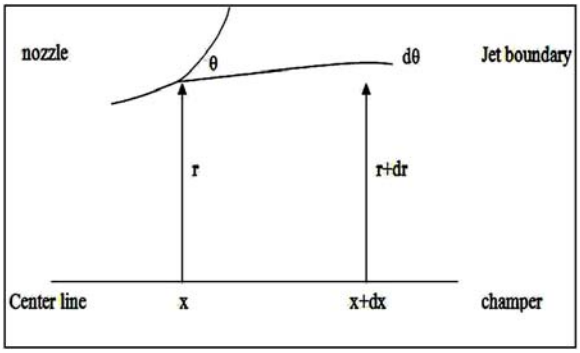

Figure 2: show the expended beam flow

$$dP = 0 = \frac{\partial P}{\partial A} + \frac{\partial P}{\partial \theta} d\theta \text{.....(6)}$$

dP =Pressure change along jet boundary

$$\frac{\partial P}{\partial A} dM + \frac{\partial P}{\partial \theta} d\theta = 0 \text{.....(7)}$$

change in area dA result in a change in mach dM for isentropic flow:

$$\theta = \left(\frac{\gamma-1}{\gamma+1}\right)^{1/2} \tan^{-1}\left(\frac{\gamma-1}{\gamma+1}\beta\right)^{1/2} - \tan^{-1}\beta - \left[\left(\frac{\gamma+1}{\gamma-1}\right)^{1/2} \tan^{-1}\left(\frac{\gamma-1}{\gamma+1}\beta\right)^{1/2} \beta \tan^{-1}\beta\right] \text{...(8)}$$

$$\beta = \sqrt{M^2 - 1}$$

θ= maximum nozzle divergence for parallel beam trajectory

4. Skimmer: For further confinement of the beam geometry, skimmer is placed at a certain position and shape to account for the following.
   a. Internal angle of the skimmer is important for absorbing the out flowing molecules to avoid shock wave formation and back scattering of molecules of the skimmer is such to reflect sideways the molecules of the tail of the incoming beam, where they would be pumped out without affecting the main stream.
   b. The distance between the nozzle and skimmer (I_s), occurs around the first mach disk of the out flowing beam to prevent shock wave and with maximum throughput as shown in equation (9) and (Figure 3).

$$\frac{r(M.D)}{\phi} = 0.67(P_o / P)^{1/2} \text{.....(9)}$$

$I_s <$ r(M.D)

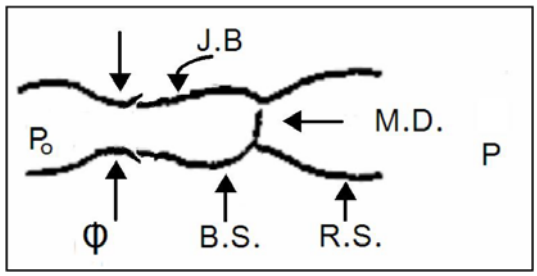

Figure 3: show flow beam with maximum throughput

J.B.: Jet boundary
M.D.: Mach disk
B.S.: Barrel shock
R.S.: Reflected shock
P_o: Pressure inside nozzle container
P: Pressure in chamber
I_s: Position between nozzle and skimmer

The above empirical equation (9) resembles the minimum distance of occurrence of mach disc.

Experiment

The throat of the nozzle was at first 2mm in diameter which was then reduced to 1mm diameter. Different operating conditions were performed i.e. operation at different temperatures and in Nitrogen hot gas injection was also attempted while heating the sodium in the nozzle.

The results was not satisfactory, it should have a broad distribution of beam velocity but narrow geometry, this because the nitrogen hot acts as a carrier to the sodium atoms with no preferential in atomic out flowing velocities.

The test points were to photograph the fluorescence of the beam due to laser atomic beam interaction as shown in Figure 4. Schlieren shadow graph technique was also considered for further indication of the beam profile.

Various nozzles were examined with divergences of 8°, 30°, 40° and 60° of which the best nozzle 5.15° was chosen according to minimum divergence of the beam.

The length of the diverging part of the nozzle was not critical. In the designed the divergence lengths were 3mm and 5mm but in both cases showed an effect on the out flowing beam.

The main set up includes the differential pumping system as shown in Figure 5.

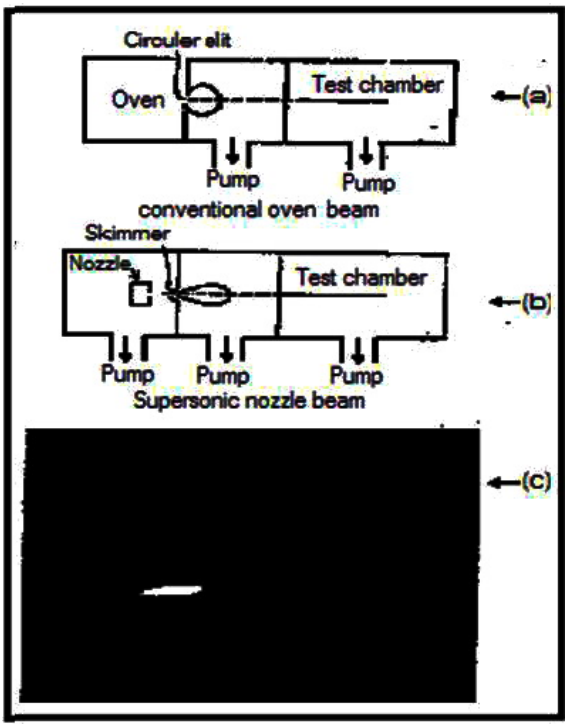

Figure 4: a. Shape of beam effusive, b. Supersonic nozzle beam, c. Photograph of laser with atomic beam fluorescence interaction

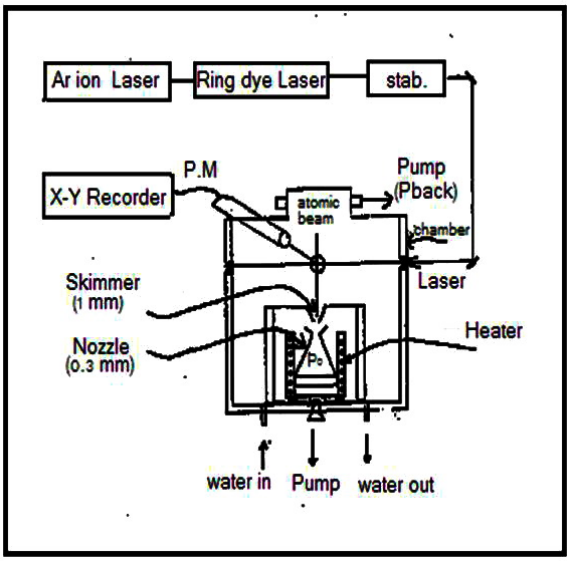

Figure 5: Schemiatic diagram showing atomic beam interacting with Ar^+ pump dye laser

Which shows the designed heater of kanthal obtained as measured by Pt/13 Rh thermocouple placed at the throat of the nozzle. More details of the nozzle are shown in Figure 6.

The water cooled jacket around the nozzle, adsorbs the plume effect of the beam that usually occurs at the nozzle and causes further scattering of the beam.

The laser part includes 171-19 type spectra physics argon ion laser pumping ring dye laser type 380D spectra physics with stabilized single frequency output CW dye laser.

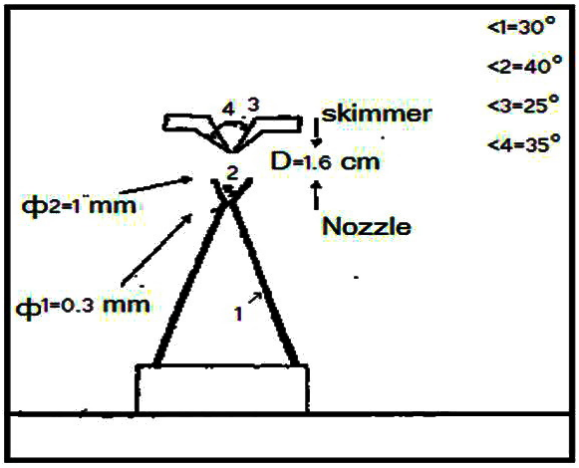

Figure 6: Details of nozzle and skimmer

The laser with node separation of 200MHz is tuned with piezo etalen free spectra range (FSR) 75 GHz, fine etalon FSR-900 GHz, and piezo mount M_2 mirror as shown in Figure 7.

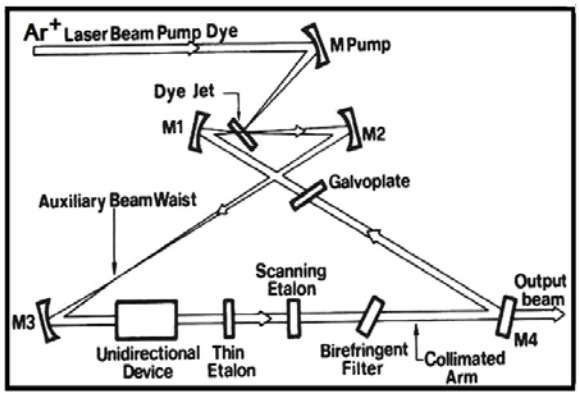

Figure 7: Ring Dye laser

The R6G dye laser was tuned to the sodium D_2 line 5895.923Å, and the wavelength was checked with a sodium reference absorption cell which shows fluorescence of the self reversible sodium line.

The laser was aligned to orthogonally interact with the Na atomic beam, the fluorescence signal was detected with an EG & G type photomultiplier, that was placed orthogonal both to the laser and Na atomic beam as shown in Figure 5. Care was taken to reduce background in the vacuum interaction chamber.

Results and Discussion

Fluorescence signal of the beam due to the 10GHz scan and interaction range of the laser with supersonic atomic beam, was detected by the photomultiplier and the signal was recorded on Xy recorded as shown in Figure 8.

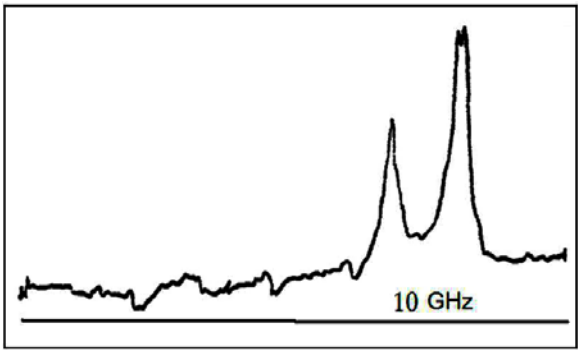

Figure 8: Spectrum of ring dye laser interaction with Na atomic beam at beam temp of 77K showing Na-D_2 line, Ring dye laser scan 10GHz, Temp of nozzle 415°C, FWHM=0.32 GHz, Width of hyperfine structure =1.03GHz.

Like wise, the cell action i.e. broader interaction region of the laser with the Na particles was also recorded and show in (Figure 9).

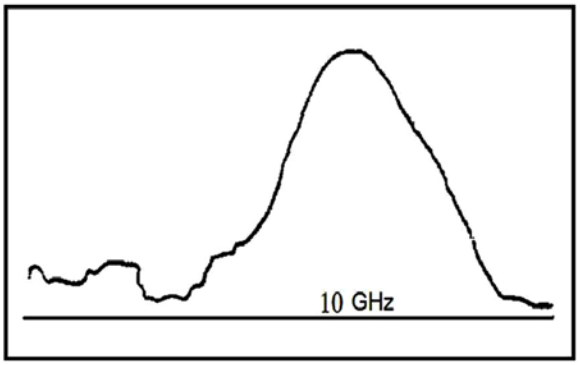

Figure 9: Spectrum of Na-cell D_2 line with ring dye laser FWHM=2.46 GHz

The results indicate a supersonic atomic beam of mach 4.855 and beam velocity 10.5×10^4 cm/sec (as calculated from equations (1) and (4), for the nozzle shown in Figure 5. The full width at half maximum width of the nozzle FWHM=0.32 GHz as compared to the cell action of 2.46GHz. The beam diverged by 5.15° as calculated from Doppler interaction of the laser beam with the supersonic atomic beam of sodium.

$$\frac{\Delta\upsilon}{\upsilon} = \frac{v\sin\theta}{c} = \frac{\Delta\upsilon}{c/\lambda}$$

$$v\sin\theta = \Delta\upsilon\lambda$$

where:

v=beam velocity, 10.5×10^4cm/s
c= velocity of light
vsinθ=component of beam velocity in the direction of the laser
Δυ= half width of beam profile =0.32/2GHz
λ= 5895.923Å ; θ=5.15°

The flux of the beam was measured by collecting the Na atoms adsorbed on a glass plate for a certain. The measured flux rate was 6.98×10^{15} part/sec. as compared to the calculated rate 9.44×10^{14} part/sec. (equation 6.) and the results are listed in Table 1.

The shift in the hyperfine structure of the Na D_2 line 5895.923Å of transition $^2p_{3/2}$-$^2s_{1/2}$ is shown in Figure 8 been measured 1.03GHz of the fluorescence laser supersonic atomic beam interaction. The shift in the hyperfine structure is the splitting of $^2s_{1/2}$ ground state of the sodium D_2-line as shown in Figure 10 [7].

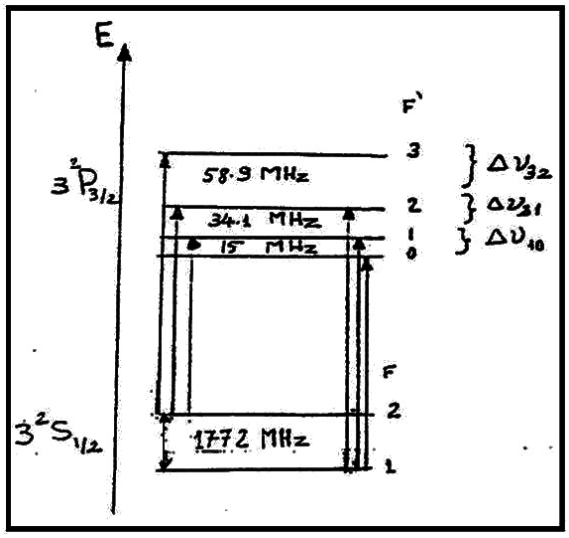

Figure 10: Part of the level scheme of sodium showing the hyperfine splitting of the 3 $^2p_{3/2}$ and the ground state 3 $^2S_{1/2}$ [7].

The hyperfine shift in sodium was found by many authors to be 1.7GHz as measured from fluorescence of laser effusive type atomic beam interaction [7], and Sodium diffusion barrier coatings prepared by sol-gel method [8].

The main difference between supersonic beams and effusive type beams (a part from the difference in flux and width of the beam), are the temperature of the atoms or molecules in the beam. The temperature calculated being 77°K as compared to room temperature (300°K) in case of effusive type beam. This effect causes sharper lines and narrower broadening [9].

The high resolution obtained allows calculation the splitting of state in term of electronic, nuclear and total angular momentum.

Where

F=I+J

The energy of the hyperfine structure is

$$W_F = W_J = \frac{C}{2}A_J + \frac{3C(C+1)-4I(I+1)J(J+1)}{8I(2I-1)J(J+1)}B_J$$

Where

C=F(F+1)-I(I+1)-J(J+1)
W_J= Energy of fine structure term.

A_J=Magnetic splitting factor
B_J=Nuclear quadruple coupling constant.

Table 1: Results with sodium Na

Mach=4.85
Flux rate (measured)=$6.98x10^{15}$part/sec
Flux rate (calculated)=$9.44x10^{14}$ part/sec
Φ=0.3mm
λmfp=0.148mm
line (FWHM)=0.32GHz
Laser of a Na line = 5895.923Å
Temp. (T_o)=415°C
T=77°K
Hyperfine structure = 1.03GHz
P_o=0.7 Torr
P_s=$3x10^{-3}$ Torr
P_b=$1x10^{-5}$ Torr

Conclusion

The difference between the nozzle supersonic beam and effusive type beam are the temperature of the atoms which was reduced to 77Kº, as compared to room temperature 300 Kº in case of effusive type beam. This effect causes shorter line and narrower broadening.

References

1. Tamsey, N. F. **1956**. *Molecular Beams*, Clarendon Press, Oxford. pp. 49-60.
2. Smith, K. F. **1995**. *Molecular Beams*, Methuen, London, p.55.
3. Shapiro, A. H. **1963**. *The dynamics and thermodynamics of compressible fluid flow*, Ronald press, New York. pp.18-25.
4. Valyi, I. **1977**. *Atomic and ionic sources*, Wiely. pp.30-32.
5. Streeter, V. L. **1975**. Handbook of fluid dynamics, Mc-Graw Hill. p.118.
6. Anderson, J. B. and Fenn, J. B. **1965**. *High energy molecular beam*, Acadmic press, New York, pp.28-35.
7. Leuchs, G. **1997**. Laser effusive type atomic beam interaction. *Opt. Comm*. **3**(1): 313-321.
8. Marek Nocun ; Dorota Burcon; Stanislaw and Siwulski **2008**. Sodium diffusion barrier coatings prepared by sol-gel method. *Optica Applicata* Vol. **XXXV111** (1):171-179.
9. Bezug, N. Lov; Ekers, A. **2008**. *Spatial contral of Na excitation*. Institute of physics Rusia. pp.1-4.